

A Study of Wet Oxidized $\text{Al}_x\text{Ga}_{1-x}\text{As}$ for Integrated Optics

A. Bek, A. Aydinli, J. G. Champlain, R. Naone, *Member, IEEE*, and N. Dagli

Abstract—An investigation of wet oxidized $\text{Al}_x\text{Ga}_{1-x}\text{As}$ layers in integrated optical applications is reported. Refractive index and thickness shrinkage of wet oxidized $\text{Al}_x\text{Ga}_{1-x}\text{As}$ layers are measured using spectroscopic ellipsometry. A Cauchy fit to the refractive index is found in the wavelength range between 0.3 and 1.6 μm . The refractive index at 1.55 μm is found to be 1.66 ± 0.01 with little dispersion around 1.55 μm . Very low loss single-mode waveguides with metal electrodes showing very low polarization dependence of loss coefficient are fabricated using wet oxidized $\text{Al}_x\text{Ga}_{1-x}\text{As}$ layers as upper cladding. Optical polarization splitters are also designed and fabricated from the same type of waveguides taking advantage of increased birefringence. Designs utilizing wet oxidized $\text{Al}_x\text{Ga}_{1-x}\text{As}$ are compared with conventional designs using only compound semiconductor heterostructures.

Index Terms—Integrated optics, optical waveguides, oxidation, polarization splitters.

I. INTRODUCTION

INTRODUCTION of oxidized $\text{Al}_x\text{Ga}_{1-x}\text{As}$ layers [1] in various electronic and optoelectronic devices has led to significant improvement in device performance. For example vertical cavity surface emitting lasers with oxidized $\text{Al}_x\text{Ga}_{1-x}\text{As}$ apertures have resulted in lower threshold currents [2]. These improvements result from a low index of refraction of insulating layers that form after wet oxidation of $\text{Al}_x\text{Ga}_{1-x}\text{As}$. The same property is also attractive for guided wave optics. Low index of refraction results in stronger optical confinement, which helps to fabricate compact devices and to reduce electrode related loss which is typically polarization dependent. Furthermore, very different boundary conditions for TE and TM polarized modes at the oxide interface increase the birefringence significantly enabling compact polarization splitters and converters.

Although this idea is attractive its feasibility needs to be investigated. The unknowns are the mechanical quality and index of refraction of wet oxidized $\text{Al}_x\text{Ga}_{1-x}\text{As}$ layers which are considerably thicker than the commonly used thickness in vertical-cavity surface-emitting lasers (VCSEL's) and

Manuscript received October 12, 1998; revised December 28, 1998. This work was supported in part by an international NSF grant, in part by a UC MICRO/Fermionics grant, in part by a NATO CRG grant. The work of A. Aydinli was supported in part by a Fulbright scholarship.

A. Bek and A. Aydinli were with the Department of Electrical and Computer Engineering, University of California, Santa Barbara, CA 93106 USA. They are now with the Department of Physics, Bilkent University, Ankara 06533, Turkey.

J. G. Champlain, R. Naone, and N. Dagli are with the Department of Electrical and Computer Engineering, University of California, Santa Barbara, CA 93106 USA.

Publisher Item Identifier S 1041-1135(99)02503-3.

metal–semiconductor field-effect transistors (MESFET's). The propagation loss of optical waveguides utilizing $\text{Al}_x\text{Ga}_{1-x}\text{As}$ and the possibility of applying voltages across oxidized $\text{Al}_x\text{Ga}_{1-x}\text{As}$ layers should also be investigated. In this letter, we present a systematic study of the feasibility of utilizing oxidized $\text{Al}_x\text{Ga}_{1-x}\text{As}$ for integrated optical applications.

II. INDEX OF REFRACTION OF OXIDIZED $\text{Al}_x\text{Ga}_{1-x}\text{As}$

We carried out a spectroscopic ellipsometry measurements of the optical constants of oxidized $\text{Al}_x\text{Ga}_{1-x}\text{As}$. The sample for spectroscopic ellipsometry consisted of single layer of 220-nm MBE-grown AlAs grown on semi-insulating GaAs. AlAs was capped by a 10-nm-thick GaAs. 100- μm -wide mesas separated by 3- μm trenches were then photolithographically defined and etched by reactive ion etching (RIE) in $\text{SiCl}_4:\text{BCl}_3$ with 30 sccm:20 sccm flow rates, respectively at 10 mTorr. 150 W of RF power was used during etching. Samples were oxidized immediately afterwards in water vapor atmosphere at 400 °C for 90 min. Water vapor was carried with N_2 gas from a glass bubbler kept at 80 °C. Due to trenches and the GaAs cap layer oxidation proceeds laterally. Trenches also help to prevent cracks in the oxidized layer due to stress. Spectroscopic ellipsometry was done in the range of 300–800 nm. A software package was used for model generated fit to the experimental data. Both as grown and oxidized samples were analyzed. A Cauchy model where the refractive index assumes a form of $n(\lambda) = A + B/\lambda^2 + c/\lambda^4$ was used to model the AlO_x layer since AlO_x is known to be transparent throughout most of the visible part of the electromagnetic spectrum [3].

The fit between the data and the model for the as grown material yielded an AlAs layer thickness of 220 nm, the GaAs cap layer thickness of 10 nm and a native oxide thickness of 1.7 nm. These values are in excellent agreement with the expected ones and the mean square error between the fit and the data was very low. The fit for the oxidized sample resulted in a total oxide thickness of 210 nm. We used an effective medium approximation to estimate the void percentage in AlO_x and to account for the presence of very narrow trenches in the oxidized film. Introduction of an unoxidized GaAs cap worsened the fit and was discarded. This implies that all of the cap is oxidized during oxidation. The refractive index obtained from the Cauchy model shows little dispersion beyond 400 nm and is extrapolated to 1600 nm. This is justified by the fact that the dispersion of the Cauchy function is very small as well as the fact that no contributions to the refractive index are expected down to very long wavelengths. The resulting refractive index values as a function of wavelength together

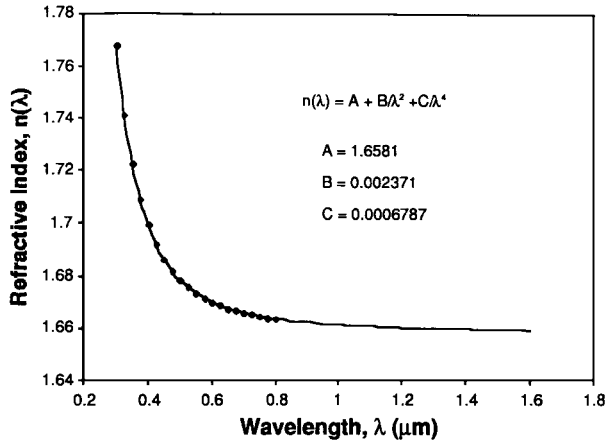


Fig. 1. Measured refractive index of oxidized AIAs as a function of wavelength. Inset shows the parameters used to fit the data to the Cauchy formula for the index of refraction.

with the Cauchy parameters A, B, and C are shown in Fig. 1. It is possible to find slightly different index and thickness fits to the measured data by modeling. The least mean-square error (mse) was lowest for the given fits, although it was somewhat larger compared to the fit for the as grown sample. This could be due to the inhomogenities in the oxidized layer and the interface with the substrate. We find that the refractive index is 1.66 ± 0.01 at 1550 nm. This number is in good agreement with the reported measured values at 632 nm [3] and 980 nm [4]. If we assume that all of the top layer including the cap and the native oxide is still present in an oxidized state on the AlO_x layer, we find a shrinkage of 9%. The void percentage estimated using effective medium approximation was about 5%.

III. LOW-LOSS OPTICAL WAVEGUIDES WITH ELECTRODES

Metal electrodes in close proximity to optical waveguides lead to excess optical propagation loss, in particular for a TM mode, due to efficient coupling between TM polarized light and surface plasmons in a metal [5]. While polarization dependent optical loss due to metal electrodes has been used to fabricate various types of polarization dependent optical devices [5], it has also hindered progress in polarization independent devices. One solution to the problem is to increase the semiconductor cladding layer thickness under the metal electrode. However, this may increase the upper layer cladding thickness significantly requiring excessive epitaxial growth time, excess applied voltage and planarization problems during fabrication. Another possibility is to introduce a low index material under the metal electrode to effectively attenuate the field before it reaches the electrode. In this work we use an oxidized $\text{Al}_x\text{Ga}_{1-x}\text{As}$ layer under the metal electrode. This approach reduces the loss and its polarization dependence while increasing the birefringence.

A schematic of the waveguides used in this work is given in Fig. 2. All epitaxial layers are undoped and grown by MBE. On these layers rib waveguides are fabricated using the same RIE and wet oxidation described earlier. Finally, after wet oxidation Ti–Pt–Au (20 nm/50 nm/500 nm) electrodes are

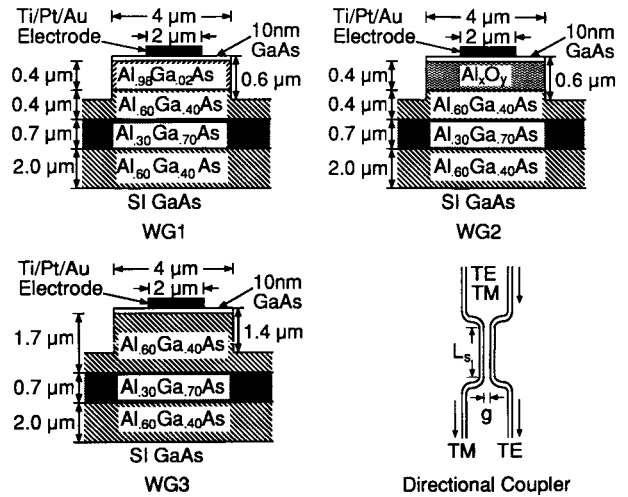


Fig. 2. Cross-sectional schematics of the waveguides and top view schematic of the directional coupler polarization splitters studied in this letter.

TABLE I
TE AND TM LOSS COEFFICIENTS AND FACET REFLECTIVITIES
OF THE WAVEGUIDES SHOWN IN FIG. 2

| | TE Loss Coefficient | TM Loss Coefficient | TE Facet Reflectivity | TM Facet Reflectivity |
|-----|---------------------|---------------------|-----------------------|-----------------------|
| WG1 | 3.7 dB/cm | 6.0 dB/cm | 0.31 | 0.23 |
| WG2 | 0.6 dB/cm | 1.0 dB/cm | 0.33 | 0.23 |
| WG3 | 1.5 dB/cm | 2.1 dB/cm | 0.31 | 0.23 |

e-beam deposited on the ribs using liftoff. High Al content for the core and the upper cladding was chosen to minimize possible stress upon oxidation of the top most cladding layer.

Propagation loss and the facet reflectivity of the rib waveguides are measured using the Fabry–Perot (FP) resonance and sequential cleaving method using the 1.55- μm output of a DFB laser. Starting length of the waveguides was 9 mm and they were cleaved into two different lengths of 6 and 3 mm. A polarization controller was used at the input. The output was collected by a 20 \times objective lens and imaged onto a camera through a polarization analyzer to confirm the correct polarization of the optical waveguide mode. A Ge detector replacing the camera was used to measure the output intensity as a function of the output wavelength. All waveguides were found to be single mode.

The results are shown in Table I. The facet reflectivity for all structures is in agreement within 3% with both existing experimental data and theoretical predictions. The loss results clearly show that 0.4- μm $\text{Al}_{0.98}\text{Ga}_{0.02}\text{As}$ layer is not thick enough to reduce the field amplitude to insignificant level at the metal electrode interface. As a result the WG1 loss coefficient is 3.7 and 6.0 dB/cm for TE and TM modes, respectively. This is especially high for TM mode as expected. On the other hand, the waveguide with oxidized $\text{Al}_{0.98}\text{Ga}_{0.02}\text{As}$ top most cladding (WG2) has dramatically lower propagation loss due to the fact that lower index of refraction of oxidized $\text{Al}_{0.98}\text{Ga}_{0.02}\text{As}$ significantly reduces the evanescent field of the propagating light on the metal electrode. The measured loss coefficients of 0.6 and 1.0 dB/cm for TE and TM polarizations,

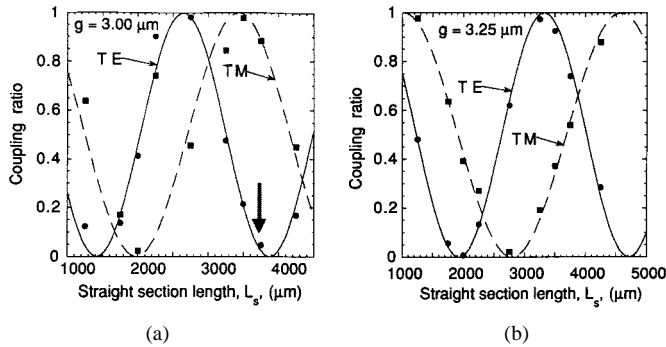


Fig. 3. Coupling ratios of directional couplers made out of WG2 for TE and TM polarizations. Arrow marks the position of the maximum extinction ratio.

respectively, for WG2 clearly demonstrate this fact. This low-loss coefficient also demonstrates the high optical quality of the oxidized $\text{Al}_{0.98}\text{Ga}_{0.2}\text{As}$ interface. It should be noted that the oxidized $\text{Al}_{0.98}\text{Ga}_{0.2}\text{As}$ thickness of $0.4 \mu\text{m}$ used in this work is significantly higher than that in previous studies. Such thick layers of oxidized $\text{Al}_{0.98}\text{Ga}_{0.2}\text{As}$ are found to be crack free and resulted in very high quality waveguides as long as 1 cm. Using a thick cladding layer under the metal as in WG3 yields propagation losses of 1.5 and 2.1 dB/cm for TE and TM modes, respectively. The TM loss coefficient is still higher indicating incomplete suppression of the field at the metal electrode interface.

IV. POLARIZATION SPLITTERS

For polarization diversity devices a common approach is to split the TE and TM parts of the incoming light and manipulate them separately. This requires integrated optical polarization splitters. A commonly used approach to fabricate such polarization splitters is to use a directional coupler with birefringent waveguides. A schematic of such a directional coupler is shown in Fig. 2. It is designed such that it is m and n coupling lengths long for TE and TM polarized inputs, respectively. m and n are integers such that $m = n + 1$. This allows one to separate the TE and TM parts of an incoming light as shown in Fig. 2. In order to realize compact polarization splitting directional couplers large waveguide birefringence is needed. The birefringence that is achievable in a compound semiconductor heterostructure is limited. On the other hand, lower oxidized $\text{Al}_x\text{Ga}_{1-x}\text{As}$ index can be used to increase waveguide birefringence. This increased birefringence is due to very different boundary conditions for TE and TM polarized modes at the oxidized $\text{Al}_x\text{Ga}_{1-x}\text{As}$ and compound semiconductor interface. Directional couplers of various lengths and gaps were fabricated out of WG2 and WG3 to investigate optical polarization splitters. TE or TM polarized light was launched from either one of the input ports and polarized light intensity at both outputs were measured. A polarization analyzer was positioned between the sample and the detector to confirm the correct polarization of the output waveguide mode. For both polarizations, the ratio of the light intensity at one of the ports to the total light intensity from both ports is plotted in Fig. 3 for couplers made out of WG2 as a function of the straight coupling section length. The power

transfer functions based on coupled-mode theory are least squares fitted to the data. There is some power transfer between the waveguides even when the length of the straight part of the coupler was zero. This is due to nonuniform coupling at the $1500 \mu\text{m}$ long, gradually curving sections at the input and output. As expected this coupling is different for both polarizations due to waveguide birefringence. We find TE/TM extinction ratios as high as 12.5 dB for a total device length of $6800 \mu\text{m}$ for the $3\text{-}\mu\text{m}$ gap coupler. It is not always possible to get a very good on/off ratio using a passive design. We intended to fine tune the coupler electronically by applying voltages between the electrodes on top of the waveguides to improve the on/off ratio. However, we were not able to create any changes for dc voltages. This is most likely due to large amount of charge trapped in and the interface of oxidized $\text{Al}_{0.98}\text{Ga}_{0.2}\text{As}$ which seems to screen the applied field. For applied voltages at 10 kHz and higher frequencies it was possible to modulate the TE polarized light by 10% for a 20-V applied voltage. This again suggests that charge screening the field has very low mobility and is most likely contained in the oxide and at the interface. In comparison, polarization splitting directional couplers made out of WG3 with much lower birefringence did not show any TE/TM selectivity for the coupler dimensions used in this letter.

V. CONCLUSION

The index of refraction and the thickness shrinkage of the AlO_x layers resulting from wet oxidation of $\text{Al}_x\text{Ga}_{1-x}\text{As}$ was measured using spectroscopic ellipsometry. Low-loss optical waveguides with metal electrodes on top where electrode related loss coefficients and their polarization dependence were decreased by as much as a factor of six was fabricated. Polarization splitting directional couplers with reasonably high extinction ratios were also fabricated taking advantage of high birefringence in waveguides containing oxidized $\text{Al}_x\text{Ga}_{1-x}\text{As}$. However, it was not possible to apply dc electric fields through thick oxidized $\text{Al}_x\text{Ga}_{1-x}\text{As}$ layers to change the index of the semiconductor part of the waveguides. Only small changes were observed for electric fields at frequencies of 10 kHz or higher.

REFERENCES

- [1] J. M. Dallesasse, N. Holonyak, A. R. Sugg, T. A. Richard, and L. El-Zein, "Hydrolyzation oxidation of $\text{Al}_x\text{Ga}_{1-x}\text{As}/\text{AlGaAs}$ quantum well heterostructures and superlattices," *Appl. Phys. Lett.*, vol. 57, no. 26, pp. 2284–2846, 1990.
- [2] H. Q. Hou, K. D. Choquette, K. M. Geib, and B. E. Hammons, "High performance $1.06 \mu\text{m}$ selective oxidized vertical cavity surface emitting lasers with $\text{InGaAs}/\text{GaAs}$ strain compensated quantum wells," *IEEE Photon. Technol. Lett.*, vol. 9, pp. 1057–1069, Aug. 1997.
- [3] A. R. Sugg, E. I. Chen, N. Holonyak, Jr., K. C. Hsieh, J. E. Baker, and N. Finnegan, "Effects of low temperature annealing on the native oxide of $\text{Al}_x\text{Ga}_{1-x}\text{As}$," *J. Appl. Phys.*, vol. 74, no. 6, pp. 3880–3885, Sept. 1993.
- [4] H. Nickel, "A detailed experimental study of wet oxidation kinetics of $\text{Al}_x\text{Ga}_{1-x}\text{As}$ layers," *J. Appl. Phys.*, vol. 78, no. 8, pp. 5201–5203, Oct. 15, 1995.
- [5] P. Albrecht, M. Hamacher, H. Heindrich, D. Hoffmann, H. P. Nolting, and C. M. Weinert, "TE/TM mode splitters on InGaAs/InP ," *IEEE Photon. Technol. Lett.*, vol. 2, pp. 114–115, Feb. 1990.